Computational Chemistry

Endocircular Li Carbon Rings

Yi-Fan Yang and Lorenz S. Cederbaum*

Abstract: *By employing accurate state-of-the-art many-electron quantum-chemistry methods, we establish that monocyclic carbon rings can accommodate Li guest atoms. The low-lying electronic states of these endocircular systems are analyzed and found to include both charge-separated states where the guest Li atom appears as a cation and the ring as an anion and encircled-electron states where Li and the ring are neutral. The electron binding energies of the encircled-electron states increase drastically at their highly symmetric equilibrium geometries with increasing size of the ring, and in Li@C$_{24}$, this state becomes the ground state. Li is very weakly bound vertical to the rings in the low-lying encircled-electron states, hinting to van-der-Waals binding. Applcations are mentioned.*

Introduction

Carbon allotropes are both simple and complex at the same time. They are simple, because they are made of only one elementary substance in relatively high symmetries.[1–3] On the other hand, they are molecules with many geometrical structures, e.g., spherical fullerenes,[4] planar graphenes,[5] cylindrical carbon nanotubes,[6] carbon cyclic rings,[7] etc. Their large variety in geometry results in intriguing complex electronic structures. For example, fullerenes can form both compacted valence bound states (hybridizing from valence orbitals), and diffuse superatomic bound states (hybridizing from higher unoccupied orbitals),[8–15] when they accept an extra electron.

Carbon rings have attracted great attention due to their connections to the formation process of other carbon allotropes.[16–20] The abundance in ion chromatography experiments[21] of carbon monocyclic rings shows the importance of studying large carbon monocyclic rings, especially even number monocyclic rings with either equal or alternating bond lengths. However, there are obstacles in studying these important allotropes. Due to the difficulty to synthesize carbon rings and to determine their structures experimentally,

theoretical approaches play an important role in determining their structures. In addtion, it is still an ongoing challenge to determine the correct energetically favorable structure of carbon rings by applying the popular density function theory (DFT).[22] Thus, to study properties of carbon rings accurately, one has to choose reliable *ab inito* methods, such as coupled-cluster method.[23]

Encapsulating or accommodating guest atoms by carbon allotropes, like fullerenes,[24] graphenes,[25] and carbon nanotubes,[26] are well-accepted ways to extend the range of applicability. We concentrate here on alkali atoms as guest atoms. There are many investigations on carbon allotropes with alkali guest atoms,[24–32] which show that they possess interesting geometrical and electronic structures and have much potential for applications. Here, we briefly mention solar cells,[33,34] superconductive agents,[35,36] and supercapacitors.[37,38] As shown in our previous accurate numerical studies, the electronic structures of endohedral alkali fullerenes vary with different sizes of carbon cages and different alkali atoms. Endohedral alkali fullerenes can form charge-separated (CS) electronic states[28,31,39–42] as well as non-charge-separated states like caged-electron (CE)[32] and split-electron (SE)[43] states. Surprisingly, to the best of our knowledge nothing is known on carbon rings encircling a guest atom like Li or other alkalies. Do such endocircular systems exist as stable entities and if yes which kind of electronic states do they support?

Our main goal is to provide answers to the above questions and to compute accurately the low-lying electronic states of Li@C$_n$ with $n = 12, 16, 20, 24$, employing state-of-the-art coupled-cluster methods. The numerical effort involved in the respective computations is rather excessive for the larger endocircular rings, but the found interesting variation of the results with the ring size justify the effort.

Results and Discussion

In the calculations we start with the ground states of the cations Li$^+$@C$_n$ ($n = 12, 16, 20, 24$) computed employing the coupled-cluster singles and doubles (CCSD)[23] method. Being closed-shell, these states suitably serve as the reference states in the calculation employing the equation-of-motion coupled-cluster method for electron affinities (EA-EOM-CCSD),[44] where the ground and excited states of the neutral Li@C$_n$ are computed by adding an electron to the reference cationic ground state. The binding energy of this excess electron (EBE) in a given state of Li@C$_n$ is by definition the energy difference between the energy of the ground state of the respective cation and that of this neutral state at a specified

[*] Dr. Y.-F. Yang, Prof. Dr. L. S. Cederbaum
Theoretical Chemistry, Institute of Physical Chemistry, Universität Heidelberg
Im Neuenheimer Feld 229, Heidelberg (Germany)
E-mail: Lorenz.Cederbaum@pci.uni-heidelberg.de

Supporting information and the ORCID identification number(s) for the author(s) of this article can be found under:
https://doi.org/10.1002/anie.202105222.

geometry, i.e., the energy gained by adding the electron at that geometry.

Considerable attention has been paid in the literature to the structure of even carbon rings.[45,46] These rings are usually divided into two types C_{4m+2} and C_{4m}, where m is an integer. The former satisfies Hückel's rule and may possess aromaticity.[47,48] Aromatic C_n rings exhibit D_{nh} symmetry, while the nonaromatic C_n rings have alternating bonds which appear in three versions[45,46] in which (i) only the bond angles alternate ($D_{\frac{n}{2}h}$ symmetry), (ii) only the bond lengths alternate ($D_{\frac{n}{2}h}$ symmetry) and (iii) both bond lengths and bond angles alternate ($C_{\frac{n}{2}h}$ symmetry). Bartlett and co-workers reported based on coupled-cluster calculations[49] that the equilibrium geometry of the ground state of the neutral C_{20} ring belongs to class (ii), i.e., D_{10h} symmetry, and similar findings can be expected for the other C_n rings we investigate here, as discussed in the literature.[50–52] To stress this issue further, we computed here the geometries of the carbon rings C_{12}, C_{16}, C_{20}, and C_{24} using the CCSD method. The results are collected in the Supporting Information (Table S3).

We start our discussion on Li@C_n by placing Li at the center of the carbon ring and optimizing the geometry of the neutral endocircular Li@C_n ($n = 12$, 16, 20, 24) systems in their electronic ground states in the respective $D_{\frac{n}{2}h}$ symmetry. Other geometrical setups and the issue of symmetry breaking will be discussed later. The optimizations and all other calculations are done using the full Dunning triple-ζ (cc-pVTZ) basis sets for the carbon[53] and lithium[54] atoms employing the CCSD and EA-EOM-CCSD theory as implemented in the CFOUR program package.[55] The results are collected in Figure S1 and Table S1 of the Supporting Information. To be able to assess the geometrical changes due to adding the excess electron to the respective cations, we have also optimized the geometry of the electronic ground states of the Li$^+$@C_n ($n = 12$, 16, 20, 24) cations in $D_{\frac{n}{2}h}$ symmetry. This has been done using the above basis sets at the CCSD level of theory. These results are also collected in the Supporting Information (Table S2).

It is illuminating to inspect the impact of inserting the guest Li atom into the center of the carbon ring. We analyze this impact in two steps. By comparing the geometries of Li$^+$@C_n in Table S2 with those of the C_n rings in Table S3, we first realize that the accommodation of the Li$^+$ cation in the center of the carbon ring has essentially a vanishing impact on the geometry of the ring. Adding now an electron to Li$^+$@C_n in order to produce the neutral Li@C_n does, however, have an impact on the C_n rings. The lengths of the C–C single bonds slightly increase and that of the triple bonds slightly decrease for $n = 12$, 16 and 20 while there is no change of the bond lengths for $n = 24$. A different behavior of Li@C_{24} from the other members of the series is also seen by inspecting the values of the bond lengths themselves. The lengths of both the C–C single and triple bonds slightly decrease when going from $n = 12$ to $n = 20$ while Li@C_{24} possesses longer single C–C bonds. The bond lengths of neutral Li@C_{24} are found to be similar to those of its cationic counterpart (see Table S1 and Table S2 in Supporting Information). The different behavior of Li@C_{24} originates from the different nature of its ground state which is discussed below.
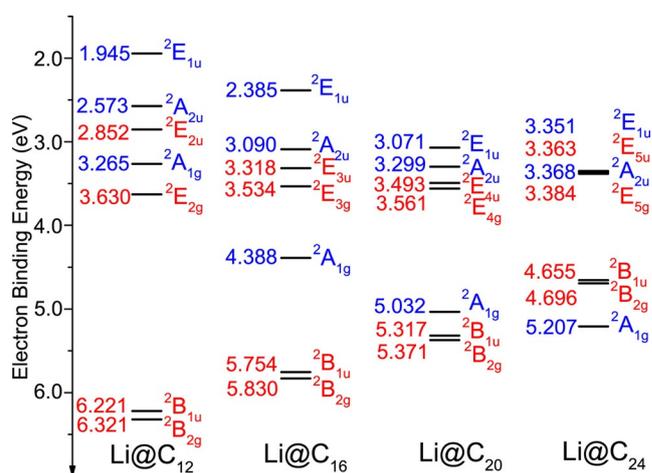
Figure 1. The binding energies of the low-lying electronic states of Li@C_n obtained at the EA-EOM-CCSD level of theory at the optimized $D_{\frac{n}{2}h}$ symmetry of the respective ground state. For more details see text. Charged-separated states are shown in red and non-charge-separated states are colored in blue.

We are now in the position to discuss the electronic states of Li@C_n. The low-lying states of Li@C_n ($n = 12$, 16, 20, 24) are collected in Figure 1. As we shall discuss below, there are two types of electronic states. Charge-separated (CS) states where the excess electron is on the carbon ring and the guest atom appears as Li$^+$ cation, and non-charge separated states where the ring stays essentially neutral and the excess electron is on the guest atom and encircled by the ring. We call the latter states encircled-electron (EE) states. The two types are shown in Figure 1 in different colors, CS states in red and EE states in blue. Interestingly, the energies of these two types show different trends. While the EBEs of the CS states either decrease or stay essentially constant, those of the EE states grow substantially with increasing ring size.

Let us first discuss the CS states. The low-lying CS states $^2B_{2g}$ and $^2B_{1u}$ of all species are nearly degenerate and their EBE reduces from about 6.3 eV for Li@C_{12} to 4.7 eV for Li@C_{24} in nearly constant steps of about 0.5 eV per additional 4 carbon atoms (slightly more for Li@C_{24} because its ground state is EE in which the ring radius is slightly larger than in the lowest CS state). The origin of this EBE-decrease is the reduction of the electrostatic interaction of Li$^+$ and the negatively charged ring in the CS states with the growing radius of the ring. To better understand the electronic structures of the $^2B_{2g}$ and $^2B_{1u}$ states and their near degeneracy, we have computed the respective singly occupied natural orbitals (SONOs) which describe the excess electron in the presence of all the electron correlations in the species. The SONOs of the CS states of Li@C_{20} are shown in Figure 2. As the CS states are similar in all systems, we chose the CS states of Li@C_{20} as an example. The electron clouds of the states resemble their counterparts in the monocyclic ring anion C_{20}^-.[50] The electron clouds of the SONOs of $^2B_{2g}$ and $^2B_{1u}$ are perpendicular to each other and since the atomic contributions overlap only little, their structure explains the near degeneracy. A few words on the higher CS states, i.e., $^2E_{au}$ and $^2E_{ag}$ ($a = 2$, 3, 4, 5). The EBEs of these states are smaller,
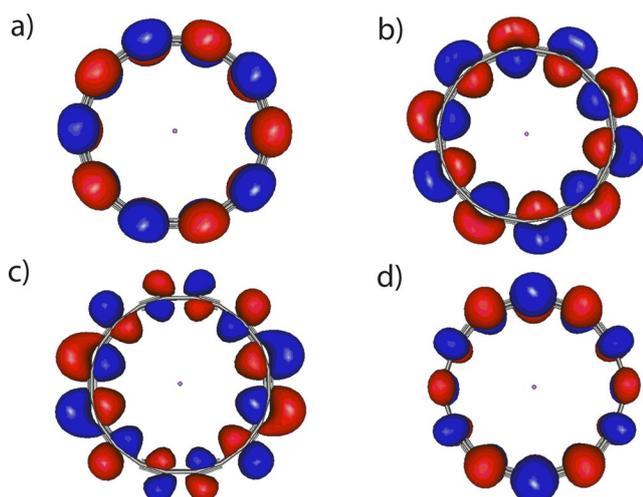
Figure 2. Image of the singly occupied natural orbitals of the low-lying charge-separated states of Li@C$_{20}$. a) $^2B_{2g}$, b) $^2B_{1u}$, c) $^2E_{4g}$, d) $^2E_{4u}$. For the $^2E_{4g}$ and $^2E_{4u}$ states, the SONOs of only one component are shown. The surfaces shown enclose 80% of the electron density.

change only slightly with the ring size and become pairwise nearly degenerate as the ring grows.

We now turn to the EE states shown in Figure 1 in blue. The EBEs are seen to increase steadily with the size of the ring encircling the excess electron. The state $^2A_{1g}$ is the state of largest EBE. In this state the binding of the excess electron increases from about 3.3 eV in Li@C$_{12}$ to about 5.2 eV in Li@C$_{24}$. The EBE is expected to increase to 5.4 eV in the Li@C$_n$ series for infinitely large n, where it becomes the binding energy of the 2s electron of the free Li atom. Interestingly, due to the increase of binding in this EE state and decrease in the CS state lowest in energy with ring size, the $^2A_{1g}$ EE state becomes the second excited state of Li@C$_{20}$ and even the ground state of Li@C$_{24}$.

In Figure 3, we collected the images of the SONOs of the $^2A_{1g}$ states of Li@C$_n$. One sees the fascinating changes of these SONOS with growing ring size. In Li@C$_{12}$, the SONO is squeezed so badly that its density looks like that of a p-type orbital although the $^2A_{1g}$ EE state is the s-type EE state
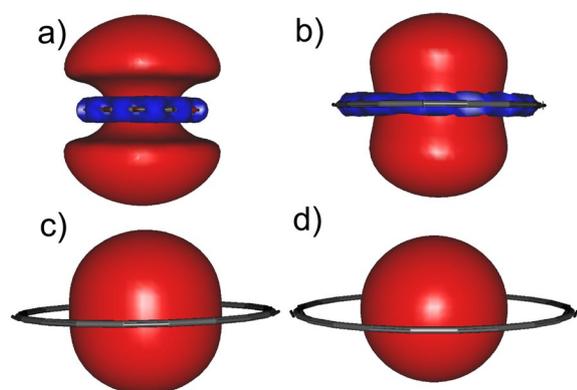
Figure 3. Image of the singly occupied natural orbitals of the encircled-electron $^2A_{1g}$ states of Li@C$_n$. a) $n=12$, b) $n=16$, c) $n=20$, d) $n=24$. The surfaces shown enclose 80% of the electron density.

stemming from the 2s orbital of atomic Li. Due to the high density outside the ring, the EBE of the corresponding state is the smallest among all the four $^2A_{1g}$ EE states of Li@C$_n$. In Li@C$_{16}$, the ring is a bit larger and the SONO corresponds to a spheroid with a narrow waist. This narrow waist is not observed in Li@C$_{20}$ and Li@C$_{24}$, due to the larger rings. The larger is the electron density near the center the larger is the EBE of the $^2A_{1g}$ state. As mentioned above, the $^2A_{1g}$ state is the s-type EE state stemming from the 2s orbital of Li. The next EE states are $^2A_{2u}$ and $^2E_{1u}$ which stem from a triply degenerate p-type orbital of Li. Being encircled by the carbon ring, the p-type EE state splits into $^2A_{2u}$ and $^2E_{1u}$ states.

Investigation of the smallest endohedral Li fullerene, the Li@C$_{20}$ fullerene, shows that the ground state is a CS state and at its optimized geometry Li$^+$ is in the center of the cage.[31] In the larger Li@C$_{60}$ endohedral fullerene the ground state is also CS, but the Li$^+$ sits off-center.[28,39,40] The first excited state of this system is a non-charge-separated state and in this state the Li guest atoms favors the central position.[32] In even larger Li endohedral fullerenes like Li@C$_{180}$, calculations indicate that the ground state has become non-charge-separated and Li again favors to be in the center of the cage.[32]

Naturally, the question arises whether symmetry breaking is to be expected for the CS and EE states of the various endocircular Li@C$_n$ systems investigated here.

To test the stability against distortion of Li of the optimized structures in D$_{\frac{n}{2}h}$ symmetry discussed above, we calculated in addition all the vibrational frequencies of the ground states at their respective optimized geometry of neutral Li@C$_n$ ($n=12, 16, 20$) at the EA-EOM-CCSD/cc-pVTZ level of theory. For completeness we also computed the vibrational frequencies of the $^2A_{1g}$ state of Li@C$_{20}$ as an example for a low-lying EE state at its own optimized D$_{\frac{n}{2}h}$ geometry. All the vibrational frequencies are shown in the Supporting Information (Table S4). The frequencies serve for the following analysis but are also of interest by themselves.

From the frequency analysis one sees that the smallest endocircular system Li@C$_{12}$ indeed possesses its energy minimum in D$_{\frac{n}{2}h}$ symmetry. This resembles the situation of the smallest endohedral Li fullerene discussed above. Obviously, moving the Li$^+$ cation away from the center leads to a distortion of the ring or cage which costs more energy than the gain by having a larger electrostatic attraction with the charged ring or cage. For the CS ground states of Li@C$_{16}$ and Li@C$_{20}$, the frequency analysis shows that the true ground state geometry is symmetry broken such that the system is planar but Li$^+$ is not in the center. What happens to the geometry of the EE states which constitute a low-lying state of Li@C$_{20}$ and even the ground state of Li@C$_{24}$, at D$_{\frac{n}{2}h}$ symmetry? The calculations of the vibrations clearly show that the ring is certainly D$_{\frac{n}{2}h}$ but the now neutral Li is very weakly attracted by the carbon ring and can move vertically out of the plane of the ring. We shall address this interesting situation below.

Computing the expected symmetry broken geometry of the CS states of the larger endocircular systems employing the EA-EOM-CCSD approach is beyond our current capabilities. To nevertheless have an idea of the resulting CS structures, we

carried out DFT calculations using the long-range corrected functional WB97XD.[56] Since the high-accuracy calculations show that Li@C$_{12}$ is of D$_{2h}$ symmetry, this system can serve as a test assessing the quality of the DFT. The geometries obtained by DFT for the lowest CS state of all systems are reported in Table S5 and shown in Figure S2 in the Supporting Information. Clearly, the Li$^+$ in the CS states is off-center and the negatively charged carbon rings are distorted to C$_s$ symmetry. This applies also to Li@C$_{12}$ which makes clear that DFT fails to reproduce the correct geometry of this system.

Due to limited computational resources, we are not able to apply the coupled cluster method to optimize the off-center geometries of Li@C$_n$. From the frequency analysis we have performed, it is clear that for $n = 16$, 20 and 24, the Li$^+$ in the CS states lowest in energy should be off-center. In the absence of better methods, we have thus used DFT to obtain the off-center optimized geometries for these states and computed their total energies and EBEs via the EA-EOM-CCSD method at these geometries. The results are collected in Figure S3 in the Supporting Information. Comparison with the energy diagram in Figure 1 shows that the symmetry breaking does only slightly stabilize the CS ground state of Li@C$_{16}$ and more that of Li@C$_{20}$ and Li@C$_{24}$, and destabilizes the EE states at the respective distorted geometries. One should keep in mind that at the optimized geometries of the EE states themselves the carbon rings are of D$_{nh}$ symmetry. At this symmetry the ground state of Li@C$_{24}$ is an EE state. At the geometry of the symmetry broken CS state lowest in energy, this EE state, of course, has a smaller EBE than at its optimized D$_{nh}$ geometry and the EBE of the CS state increases and this state becomes the global ground state (see Table S8 in the Supporting Information).

Let us return to the ^{2}A$_{1g}$ EE state of Li@C$_{20}$. As mentioned above, this low-lying state is the second excited state of the system and at its optimized geometry the carbon ring possesses D$_{nh}$ symmetry while the neutral Li guest atom is very weakly bound to the ring. To better understand the nature of the states, we performed a potential energy surface scan of the three lowest in energy states of Li@C$_{20}$ along the vertical out-of-plane direction starting at the planar equilibrium geometry of the ^{2}A$_{1g}$ EE state. The results drawn in Figure 4 show that the Li guest atom in the EE state can nearly freely move vertically out of the carbon ring plane. The EA-EOM-CCSD calculations predict that the equilibrium distance of Li from the plane is 0.28 Å and the dissociation energy breaking the Li-ring bond to be around 0.07 eV (see Supporting information, section S5). A similar situation is to be expected for the ^{2}A$_{1g}$ EE state of Li@C$_{24}$.

Conclusion

Similar to other carbon allotopes, monocyclic rings can accommodate guest atoms such as Li. The low-lying electronic states are the relevant states, which determine the chemical activity of systems, have been accurately computed for the endocircular Li@C$_n$ ($n = 12$, 16, 20, 24) compounds and found to possess interesting properties. Two kinds of states are
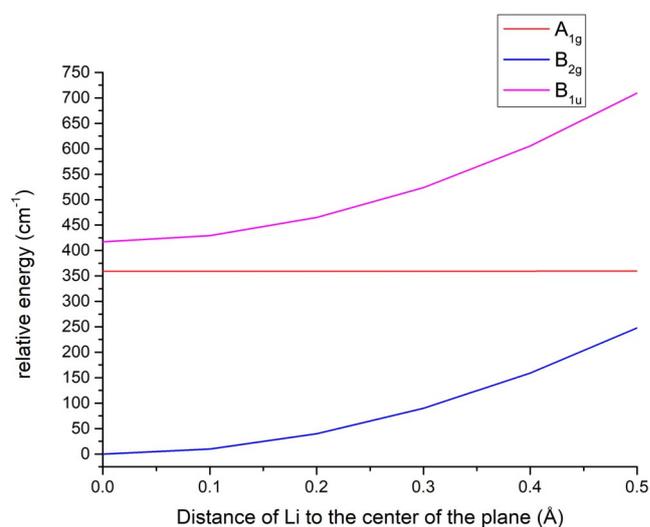
Figure 4. Potential energy surface cuts along the A$_{2u}$ mode which describes the motion of the Li atom vertical to the plane. Shown are the cuts for the three lowest in energy states of Li@C$_{20}$, a) ground state ^{2}B$_{2g}$, b) first excited state ^{2}A$_{1g}$ and c) second excited state ^{2}B$_{1u}$. At the starting point, the geometry is the planar equilibrium geometry of the encircled-electron ^{2}A$_{1g}$ state of the Li@C$_{20}$ (D$_{10h}$ symmetry). It is seen that at this geometry the three states are nearly degenerate and that the Li atom can essentially move freely vertical to the plane in the ^{2}A$_{1g}$ encircled-electron state. At the minimum of its energy, the out-of-plane distance of Li is 0.28 Å and Li is bound to the carbon ring by Van der Waals bonding. Energies (cm^{-1}) are relative to that at the D$_{10h}$ minimum.

present in the series: charge-separated with Li$^+$ cation encircled by the negatively charged ring, and encircled-electron states where a neutral Li is embedded in the ring. When the ring is small, the electrostatic interaction between Li$^+$ and C$_n^-$ is large favoring CS states. In addition, the outer valence electron of Li is strongly squeezed by the ring which disfavors EE states. With increasing radius of the ring and Li in its center, the electrostatic attraction and the squeezing decrease. As a result, the electron cloud of the encircled Li valence electron states becomes more spherical stabilizing the EE state. At the same time, the CS states destabilize and the energy gap between the CS ground state and the lowest in energy EE state reduces. In Li@C$_{24}$, the encircled-electron state then already becomes the ground state. Off-center Li leads to distorted rings favoring, of course, the CS state which at such an optimized structure is found to be the global ground state.

The very different nature of the CS and EE electronic states calls for applications. In the CS state the guest atom is strongly bound to the ring as it lost an electron to the ring and appears as Li$^+$ interacting electrostatically with the negatively charged ring. In the EE state, the Li is neutral and we have shown that it is very weakly bound to the ring by Van der Waals forces. Let us take Li@C$_{20}$ as an example. In its ground state its structure is symmetry broken, the Li$^+$ is off-center and the carbon ring distorted. If one excites the system, for instance by a laser, to the second excited electronic state which is an EE state, the ring undergoes a structural transition to a highly symmetric D$_{10h}$ structure and a neutral Li atom is

released from the system. In this way, the system can be used as a Li donor to neighboring systems which can undergo a reaction with this Li or bind it. We anticipate that a similar behavior is also taking place if the endocircular Li@C_{20} is embedded in a suitable environment. We briefly mention that the capacity to insert and extract Li is an important property for Li-Ion batteries[57–59] and hope that the present investigation sheds additional light on the possibilities to bind and emit Li atoms.

Conflict of interest

The authors declare no conflict of interest.

Keywords: ab initio calculations · monocyclic carbon rings · donor–acceptor systems · electron transfer · guest atoms

[1] R. B. King, *J. Math. Chem.* **1998**, *23*, 197–227.
[2] A. C. Tang, F. Q. Huang, R. Z. Liu, *Phys. Rev. B* **1996**, *53*, 7442–7450.
[3] Y. Cai, H. Wang, S. Xu, Y. Hu, N. Liu, X. Xu, *AIP Adv.* **2016**, *6*, 065225.
[4] H. W. Kroto, J. R. Heath, S. C. O'Brien, R. F. Curl, R. E. Smalley, *Nature* **1985**, *318*, 162–163.
[5] A. H. Castro Neto, F. Guinea, N. M. R. Peres, K. S. Novoselov, A. K. Geim, *Rev. Mod. Phys.* **2009**, *81*, 109–162.
[6] V. Schroeder, S. Savagatrup, M. He, S. Lin, T. M. Swager, *Chem. Rev.* **2019**, *119*, 599–663.
[7] H. Prinzbach, A. Weiler, P. Landenberger, F. Wahl, J. Wörth, L. T. Scott, M. Gelmont, D. Olevano, B. v. Issendorff, *Nature* **2000**, *407*, 60–63.
[8] M. Feng, J. Zhao, H. Petek, *Science* **2008**, *320*, 359–362.
[9] J. Zhao, M. Feng, J. Yang, H. Petek, *ACS Nano* **2009**, *3*, 853–864.
[10] J. O. Johansson, E. E. B. Campbell, *Chem. Soc. Rev.* **2013**, *42*, 5661–5671.
[11] V. K. Voora, L. S. Cederbaum, K. D. Jordan, *J. Phys. Chem. Lett.* **2013**, *4*, 849–853.
[12] S. Klaiman, E. V. Gromov, L. S. Cederbaumm, *J. Phys. Chem. Lett.* **2013**, *4*, 3319–3324.
[13] S. Klaiman, E. V. Gromov, L. S. Cederbaum, *Phys. Chem. Chem. Phys.* **2014**, *16*, 13287–13293.
[14] E. V. Gromov, S. Klaiman, L. S. Cederbaum, *Phys. Chem. Chem. Phys.* **2016**, *18*, 10840–10845.
[15] Y.-F. Yang, S. Klaiman, E. V. Gromov, L. S. Cederbaum, *Phys. Chem. Chem. Phys.* **2018**, *20*, 17434–17441.
[16] G. Von Helden, N. G. Gotts, M. T. Bowers, *Nature* **1993**, *363*, 60–63.
[17] J. Hunter, J. Fye, M. F. Jarrold, *Science* **1993**, *260*, 784–786.
[18] M. A. Wilson, L. S. K. Pang, G. D. Willett, K. J. Fisher, I. G. Dance, *Carbon* **1992**, *30*, 675–693.
[19] C.-H. Kiang, *J. Chem. Phys.* **2000**, *113*, 4763–4766.
[20] A. Van Orden, R. J. Saykally, *Chem. Rev.* **1998**, *98*, 2313–2358.
[21] G. von Helden, P. R. Kemper, N. G. Gotts, M. T. Bowers, *Science* **1993**, *259*, 1300–1302.
[22] É. Brémond, Á. J. Pérez-Jiménez, C. Adamo, J. C. Sancho-García, *J. Chem. Phys.* **2019**, *151*, 211104.
[23] G. D. Purvis III, R. J. Bartlett, *J. Chem. Phys.* **1982**, *76*, 1910–1918.
[24] Y. Kawashima, K. Ohkubo, S. Fukuzumi, *J. Phys. Chem. A* **2012**, *116*, 8942–8948.
[25] G. Colherinhas, E. E. Fileti, V. V. Chaban, *J. Phys. Chem. Lett.* **2015**, *6*, 302–307.
[26] G. E. Froudakis, *Nano Lett.* **2001**, *1*, 531–533.
[27] Y. Matsuo, *Bull. Chem. Soc. Jpn.* **2021**, *94*, 1080–1089.
[28] M. Stefanou, H. J. Chandler, B. Mignolet, E. Williams, S. A. Nanoh, J. Thompson, F. Remacle, R. Schaub, E. E. B. Campbell, *Nanoscale* **2019**, *11*, 2668–2678.
[29] W. Liu, Y. H. Zhao, Y. Li, Q. Jiang, E. J. Lavernia, *J. Chem. Phys. C* **2009**, *113*, 2028–2033.
[30] Y. Zhou, W. Chu, F. Jing, J. Zheng, W. Sun, Y. Xue, *Appl. Surf. Sci.* **2017**, *410*, 166–176.
[31] Y.-F. Yang, E. V. Gromov, L. S. Cederbaum, *J. Chem. Phys.* **2019**, *151*, 114306.
[32] Y.-F. Yang, E. V. Gromov, L. S. Cederbaum, *J. Phys. Chem. Lett.* **2019**, *10*, 7617–7622.
[33] C. J. Brabec, N. S. Sariciftci, J. C. Hummelen, *Adv. Funct. Mater.* **2001**, *11*, 15–26.
[34] I. Jeon, H. Ueno, S. Seo, K. Aitola, R. Nishikubo, A. Saeki, H. Okada, G. Boschloo, S. Maruyama, Y. Matsuo, *Angew. Chem. Int. Ed.* **2018**, *57*, 4607–4611; *Angew. Chem.* **2018**, *130*, 4697–4701.
[35] G. Profeta, M. Calandra, F. Mauri, *Nat. Phys.* **2012**, *8*, 131–134.
[36] Y. Kubozono, R. Eguchi, H. Goto, S. Hamao, T. Kambe, T. Terao, S. Nishiyama, L. Zheng, X. Miao, H. Okamoto, *J. Phys. Condens. Matter* **2016**, *28*, 334001.
[37] J.-H. Choi, B.-S. Kim, *Sustainable Energy Fuels* **2021**, *5*, 1988–1994.
[38] H. Wang, X. Yan, G. Piao, *Electrochim. Acta* **2017**, *231*, 264–271.
[39] M. Pavanello, A. F. Jalbout, B. Trzaskowski, L. Adamowicz, *Chem. Phys. Lett.* **2007**, *442*, 339–343.
[40] T. Debnath, J. K. Saha, T. Banu, T. Ash, A. K. Das, *Theor. Chem. Acc.* **2016**, *135*, 167.
[41] H. Ueno, S. Aoyagi, Y. Yamazaki, K. Ohkubo, N. Ikuma, H. Okada, T. Kato, Y. Matsuo, S. Fukuzumi, K. Kokubo, *Chem. Sci.* **2016**, *7*, 5770–5774.
[42] H. Ueno, I. Jeon, H. Lin, A. Thote, T. Nakagawa, H. Okada, S. Izawa, M. Hiramoto, H. Daiguji, S. Maruyama, Y. Matsuo, *Chem. Commun.* **2019**, *55*, 11837–11839.
[43] Y.-F. Yang, L. S. Cederbaum, *Phys. Chem. Chem. Phys.* **2021**, *23*, 11837–11843.
[44] M. Nooijen, R. J. Bartlett, *J. Chem. Phys.* **1995**, *102*, 3629–3647.
[45] S. Arulmozhiraja, T. Ohno, *J. Chem. Phys.* **2008**, *128*, 114301.
[46] T. Heaton-Burgess, W. Yang, *J. Chem. Phys.* **2010**, *132*, 234113.
[47] A. Karton, V. S. Thimmakondu, *Chem. Phys. Lett.* **2018**, *706*, 19–23.
[48] K. Kaiser, L. M. Scriven, F. Schulz, P. Gawel, L. Gross, H. L. Anderson, *Science* **2019**, *365*, 1299–1301.
[49] Y. Jin, A. Perera, V. F. Lotrich, R. J. Bartlett, *Chem. Phys. Lett.* **2015**, *629*, 76–80.
[50] Y.-F. Yang, L. S. Cederbaum, *J. Chem. Phys.* **2020**, *152*, 244307.
[51] W. An, N. Shao, S. Bulusu, X. C. Zeng, *J. Chem. Phys.* **2008**, *128*, 084301.
[52] V. I. Baranovski, *Chem. Phys. Lett.* **2005**, *408*, 429–432.
[53] T. H. Dunning, Jr., *J. Chem. Phys.* **1989**, *90*, 1007–1023.
[54] B. P. Prascher, D. E. Woon, K. A. Peterson, T. H. Dunning, A. K. Wilson, *Theor. Chem. Acc.* **2011**, *128*, 69–82.
[55] J. F. Stanton, J. Gauss, L. Cheng, M. E. Harding, D. A. Matthews, P. G. Szalay, CFOUR, Coupled-Cluster techniques for Computational Chemistry, a quantum-chemical program package. With

[56] J. Chai, M. Head-Gordon, *Phys. Chem. Chem. Phys.* **2008**, *10*, 6615–6620.

[57] J. B. Goodenough, Y. Kim, *Chem. Mater.* **2010**, *22*, 587–603.

[58] J. B. Goodenough, K.-S. Park, *J. Am. Chem. Soc.* **2013**, *135*, 1167–1176.

[59] X. Fan, W. T. Zheng, J.-L. Kuo, D. J. Singh, *ACS Appl. Mater. Interfaces* **2013**, *5*, 7793–7797.